

## Phase locking a clock oscillator to a coherent atomic ensemble

R. Kohlhaas<sup>1,2</sup>, A. Bertoldi<sup>3,\*</sup>, E. Cantin<sup>3,4</sup>, A. Aspect<sup>1</sup>, A. Landragin<sup>2</sup>, and P. Bouyer<sup>1,3</sup>

<sup>1</sup>*Laboratoire Charles Fabry, Institut d'Optique, CNRS, Université Paris-Sud, avenue Augustin Fresnel, F-91127 Palaiseau, France*

<sup>2</sup>*LNE-SYRTE, Observatoire de Paris, CNRS and UPMC, 61 avenue de l'Observatoire, F-75014 Paris, France*

<sup>3</sup>*Laboratoire Photonique, Numérique et Nanosciences - LP2N Université Bordeaux - IOGS - CNRS: UMR 5298, rue Mitterrand, F-33400 Talence, France*

<sup>4</sup>*Quantel, 4 rue Louis de Broglie, Building D, F-22300 Lannion, France*

(Dated: August 20, 2018)

The sensitivity of an atomic interferometer increases when the phase evolution of its quantum superposition state is measured over a longer interrogation interval. In practice, a limit is set by the measurement process, which returns not the phase, but its projection in terms of population difference on two energetic levels. The phase interval over which the relation can be inverted is thus limited to the interval  $[-\pi/2, \pi/2]$ ; going beyond it introduces an ambiguity in the read out, hence a sensitivity loss. Here, we extend the unambiguous interval to probe the phase evolution of an atomic ensemble using coherence preserving measurements and phase corrections, and demonstrate the phase lock of the clock oscillator to an atomic superposition state. We propose a protocol based on the phase lock to improve atomic clocks limited by local oscillator noise, and foresee the application to other atomic interferometers such as inertial sensors.

PACS numbers: 95.55.Sh,42.62.Eh,67.85.-d,37.25.+k

From the first observations of Huygens on the coordinated motion of coupled nonlinear oscillators [1], phase synchronization has evolved to an indispensable tool for time and frequency metrology and starts to be investigated for quantum systems [2–4]. Phase lock loops (PLLs) [5], where a local oscillator (LO) is phase locked to a reference signal, are widely used for the generation of atomic time scales [6, 7], the synchronization in telecommunication [8] or in radio navigation [9]. In usual atomic frequency standards, however, only the frequency of the local oscillator is locked on the atomic resonance. This feature derives from the quantum nature of the reference system, *i.e.*, the quantum superposition of two internal states of an ensemble of atoms, molecules or ions, which is destroyed by the detection at the end of the interrogation process. A similar limitation exists for any measurement of a quantum system as in magnetometers or inertial sensors [10]. Locking the phase of the local oscillator onto the phase of the quantum superposition of the two levels of the quantum system would improve the long term stability, as the phase is the integral of the frequency, and reduce the constraints on the stability of the LO or of the measured signal. More in general, phase locking a classical system to a quantum system would give a direct link in metrology to the fundamental oscillations of quantum particles and could lead to enhanced sensitivities and new applications in precision measurements. Here, we demonstrate the direct phase lock of a LO to an atomic ensemble, based on repeated coherence preserving measurements of the atomic ensemble. We also study how this technology could improve atomic clocks subject

to local oscillator noise.

In an atomic clock, the frequency of a LO is repeatedly referenced to an atomic transition frequency by comparing their respective phase evolutions in an interrogation time  $T$  and applying a feedback correction. During the interrogation, the atoms are in a superposition state, and the projection of the relative phase between the LO and the atomic ensemble is measured as a population imbalance of the two clock levels. The readout is thus a sinusoidal function of the phase drift, and the latter can only be unambiguously determined if it stays within the  $[-\pi/2, \pi/2]$  interval, hereafter called inversion region. Hence, for a given LO noise, the interrogation time of the atomic transition must be kept short enough such that phase drifts beyond the inversion region are avoided. Currently, LO noise limits the interrogation time in ion [11] and optical lattice clocks [12–15] and is expected to become a limit for microwave clocks with the recently discovered spin-self rephasing effect [16]. The standard approach to tackle this issue consists in improving the quality of local oscillators [17–21]. As an alternative, it has been recently proposed to track and stabilize the LO phase evolution using several atomic ensembles probed with increasing interrogation time [22, 23], or by enhancing the Ramsey interrogation interval by stabilizing the LO either via cascaded frequency corrections [24] or by coherence preserving measurements on the same atomic ensemble and feedback [25, 26].

In this letter we show for the first time how the phase lock of a classical oscillator to an atomic superposition state can be exploited to keep the relative phase between the LO and the atomic system in the inversion region. In addition, we demonstrate a protocol based on this phase lock to operate an atomic clock beyond the limit set by the LO decoherence, which nowadays represents the bot-

---

\*Electronic address: andrea.bertoldi@institutoptique.fr

tleneck of the best available frequency standards. We begin with a minimally destructive measurement of the LO phase drift when it is within the inversion region; the measurement readout is then used to correct the LO phase so as to reduce its drift. The cycle is repeated using the residual atomic coherence. The result is a series of successive, phase-related measurements of the relative phase evolution, and the feedback keeps the phase in the inversion region, leading to an effectively longer interrogation time [27]. We demonstrate this approach with a trapped ensemble of neutral atoms probed on a microwave transition.

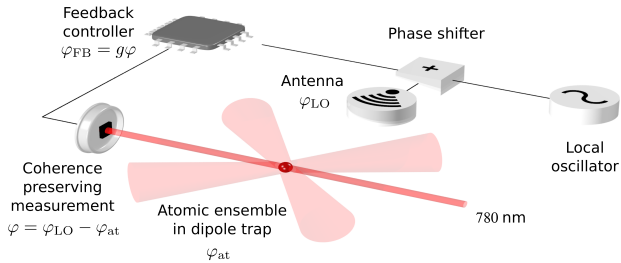


FIG. 1: **Experimental scheme.** The evolution of the LO phase  $\varphi_{LO}$  is compared to the phase  $\varphi_{at}$  of an atomic ensemble in a superposition state using coherence preserving measurements in a Ramsey spectroscopy sequence. The relative phase is obtained from the read out of the population difference, and is used to implement the phase lock between the two oscillators by applying a feedback correction phase  $\varphi_{FB}$  on the LO output using a phase actuator. The light shift induced by the optical trap and by the probe has been engineered to have a homogeneous measurement of the atomic ensemble [28].

The experimental scheme shown in Fig. 1 has been described in [28]. A cloud of cold  $^{87}\text{Rb}$  atoms is trapped in an optical potential (see Appendix A), prepared with a  $\pi/2$  pulse of a resonant microwave field in a balanced superposition state of two hyperfine levels  $|\downarrow\rangle \equiv |F=1, m_F=0\rangle$  and  $|\uparrow\rangle \equiv |F=2, m_F=0\rangle$  of the electronic ground state, and probed using a nondestructive detection. Typically,  $5 \times 10^5$  atoms at a temperature of  $10 \mu\text{K}$  are used in the measurements reported here. The phase  $\varphi_{at}$  of the superposition state oscillates at a frequency of 6.835 GHz corresponding to the energy difference between the  $|\downarrow\rangle$  and  $|\uparrow\rangle$  atomic states, which is the fundamental reference if atoms are protected from perturbations. A microwave LO has a frequency close to the atomic frequency difference, so that the relative phase  $\varphi = \varphi_{LO} - \varphi_{at}$  between the two oscillators drifts slowly because of the LO noise.  $\varphi$  can be measured using the Ramsey spectroscopy method (see Fig. 2): a second  $\pi/2$  microwave pulse (projection pulse) maps it onto a population difference, which we read out with a weak optical probe perturbing the atomic quantum state only negligibly and preserving the ensemble coherence [28–30]. Unlike for destructive measurements, the interrogation of  $\varphi$  can continue in a correlated way, once the action of the projection pulse is inverted using an oppo-

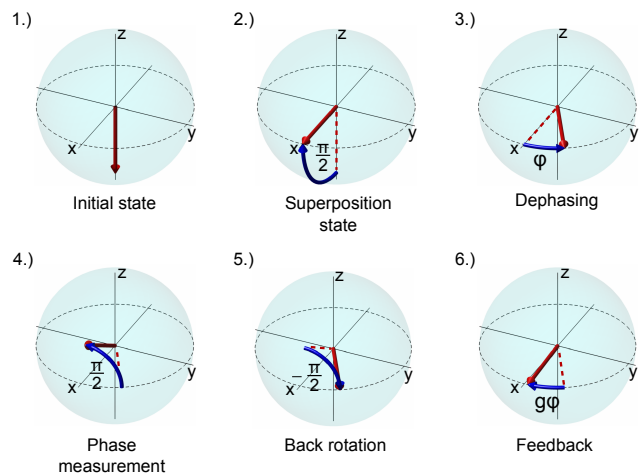
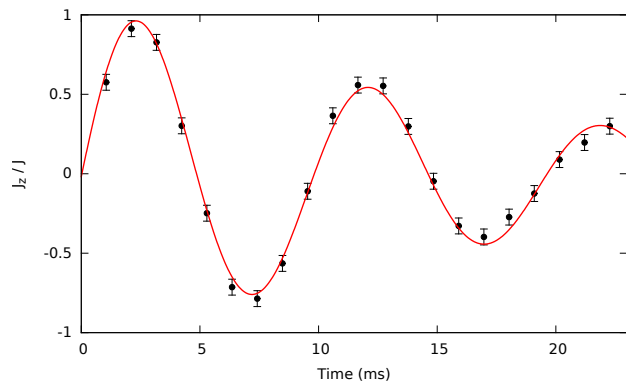


FIG. 2: **Bloch's sphere representation of the phase lock between the LO and the atomic superposition state.** The phase lock between the classical oscillator and the atomic spin is obtained using repeated, time correlated Ramsey interrogations and feedback. The sequence begins by preparing the atomic CSS in the  $|\downarrow\rangle$  state via optical pumping (step 1.). The measurement of the relative phase between the CSS and the LO starts when a  $\pi/2$  microwave pulse around the  $y$  axis brings the CSS into a balanced superposition of the  $|\downarrow\rangle$  and  $|\uparrow\rangle$  states, depicted as a vector on the equatorial plane of the Bloch sphere (step 2.). The  $x$  axis is chosen to represent the phase of the local oscillator, and  $\varphi$  the relative phase between the LO and the atomic superposition that evolves because of the LO noise (step 3.). After an interrogation time  $T$ , the projection of  $\varphi$  is mapped onto a population difference by a projection  $\pi/2$  pulse around the  $x$  axis and read out with the coherence preserving detection (step 4.). The CSS is rotated back to the equatorial plane by a reintroduction  $\pi/2$  pulse around the  $x$  axis (step 5.), and feedback is applied on the phase of the LO (step 6.). The PLL between the LO and the atomic ensemble consists in the repetition of the steps from 3.) to 6.), potentially till the atomic ensemble shows a residual coherence.

site  $\pi/2$  microwave pulse (reintroduction pulse), which brings the atomic state back to the previous coherent superposition. Moreover, after each measurement and reintroduction pulse, the phase read out can be used to correct the LO phase. The evolution and manipulation of the atomic ensemble can be illustrated using the Bloch sphere representation (Fig. 2): the collective state of  $N_{at}$  two-level atoms in the same pure single particle state (also called coherent spin state (CSS)) forms a pseudo-spin with length  $J = N_{at}/2$ , where  $J_z$  denotes the population difference and  $\varphi = \arcsin(J_y/J_x)$  is the phase difference between the phase of the LO and that of the superposition state. A resonant microwave pulse determines the rotation of  $\mathbf{J}$  around an axis in the equatorial plane of the Bloch sphere, and the axis direction is set by the phase of the microwave signal. The repetition of the manipulation, measurement and feedback cycle implements the phase lock of the LO on the atomic

superposition state, as shown in steps 2.-6. of Fig. 2.

We first show that we can reconstruct the time evolution of the relative phase between the LO and the CSS by monitoring the population difference and without applying feedback. For this purpose, we frequency offset the LO by 100 Hz from the nominal resonance, and periodically measure the projection of the relative phase  $\sin(\varphi)$  with only a small reduction of the atomic ensemble coherence (Fig. 3). Every 1 ms  $\varphi$  is mapped to a population difference via a projection  $\pi/2$  microwave pulse around the x-axis, a weak measurement of  $J_z$  is performed, and the collective spin is rotated back to the equatorial plane of the Bloch sphere via a reintroduction  $\pi/2$  pulse around the x-axis. The  $\pi/2$  microwave pulses are derived from an amplified version of the LO at 6.835 GHz leading to a pulse length of  $\tau_{\pi/2}=47 \mu\text{s}$ , and the rotation axis is controlled with a quadrature phase shifter. The coherence preserving, dispersive measurement relies on frequency modulation spectroscopy (see Appendix B). Fig. 3 shows in a single experimental run how the spin state evolves around the equator of the Bloch sphere, with the relative phase  $\varphi$  mapped on the normalized population difference  $J_z/J$ . The signal-to-noise-ratio (SNR) of the weak measurements is 20 for a full state coherence and each readout of the relative phase drift reduces the state coherence by 2%. The destructivity from the probe is the main decoherence source till 10 ms, then the inhomogeneous light shift of the dipole trap on the clock states becomes the dominant decoherence source.



**FIG. 3: Coherence preserving measurement of the relative phase between the LO and the atomic superposition.** Real-time measurement of the normalized population difference to which the relative phase  $\varphi$  between the local oscillator and the atomic superposition state is periodically mapped via microwave rotation pulses. The phase precession is induced by setting the LO frequency 100 Hz off the nominal atomic transition frequency. The experimental points are fitted with a sinusoidal evolution, damped because of the decoherence induced by the  $J_z$  measurement and the residual differential light shift on the clock transition.

We next introduce feedback and demonstrate that we can phase lock the LO on the atomic superposition state, and increase the Ramsey interrogation time beyond the

limit set by the inversion region between  $J_z$  and the relative phase. We apply on the local oscillator two types of signals, first a frequency offset, and second periodic phase jumps, and use the output of the coherence preserving measurements to actively minimize  $\varphi$ . The phase lock is obtained by controlling the phase of the local oscillator by means of a digital phase shifter (see Appendix D). The feedback is performed after the atomic spin is rotated back to the equatorial plane of the Bloch sphere. When the disturbance applied on the local oscillator consists of a frequency offset, there is a linear phase drift between the LO and the atomic phase (Fig 4, red). The phase evolution in open loop is reconstructed from the data of Fig. 3 by taking into account the damping on the sinusoidal signal due to the decoherence sources, and knowing that a constant frequency offset is applied on the LO. We remark that sudden sign inversions of the applied frequency offset when  $\varphi = \pm\pi/2$  would produce exactly the same evolution of the population difference, illustrating the need to keep  $\varphi$  in the inversion region. In closed loop, the phase drift due to the 100 Hz frequency offset on the LO is periodically reset to zero, with a precision set by the  $\pi/32$  step size of the digital phase shifter and the uncertainty of the coherence preserving measurements. As a consequence, the  $J_z/J$  signal shows a saw-tooth-like evolution (Fig. 4, blue signal). Without phase lock, the phase drift leaves the inversion region after 2.5 ms and rotates several times around the Bloch sphere, whereas with phase lock it stays in the inversion region for all the 22 ms interval shown in the image. When the feedback is active the total phase drift results as the phase measured at the end of the Ramsey interferometer, added to the correction phase shifts on the LO via the feedback controller. We next apply periodic phase jumps of  $\pi/3$  back and forth on the LO using a second phase shifter. The signal obtained in open loop is shown at the top of Fig. 5. When the feedback controller is active, the jumps detected on the relative phase are corrected to zero, with a precision set by the resolution of the phase shifter and the uncertainty of the weak measurements (Fig. 5, bottom). The solid lines in Fig. 4 and 5 are drawn from the known timing for the applied phase signal and the feedback on the phase. For a combination of a phase drift and phase jumps, the relative phase can leave the inversion region while the noise action cannot be predicted from previous measurements. This problem affects atomic clocks and highlights the requirement of feedback on the LO phase to keep track of the relative phase drifts. Without feedback, the Ramsey interrogation time should be kept sufficiently short to avoid ambiguities for the measured phase shift.

We propose now a protocol to efficiently use the phase lock to improve an atomic clock. In a conventional atomic clock, the phase drift  $\varphi$  is destructively read out after a single interrogation and feedback is performed on the LO by the addition of a feedback correction frequency  $\omega_{\text{FB}} = -\varphi/T$  considering unity gain. Our protocol of using the PLL between the LO and the atomic superpo-

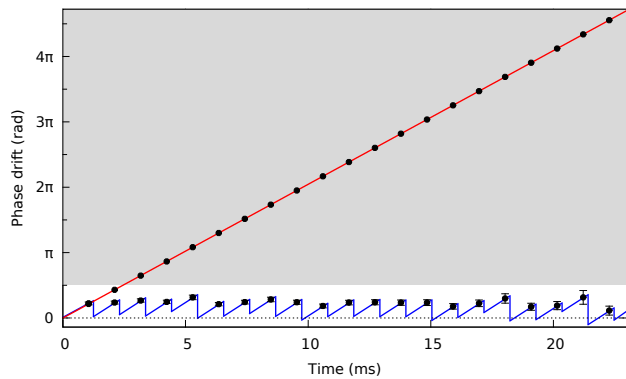


FIG. 4: **Phase lock between the LO and the atomic superposition state.** The evolution of the LO-atom relative phase is reconstructed from the  $J_z$  signal in Fig. 3 (red, solid line) and when feedback is applied on the phase of the LO after each measurement (blue, solid line). In the open loop case, the points are reported at the values given by the fit in the previous figure. In the closed loop case, the relative phase is always smaller than  $\pi/2$ , and does not enter in the region represented in grey where it cannot be univocally determined from the measurement.

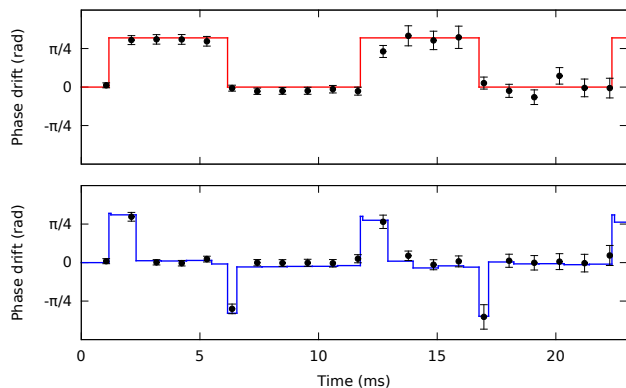


FIG. 5: **Correction of phase jumps between the LO and the atomic ensemble.** Evolution of the LO-CSS phase when periodic phase jumps of  $\pi/3$  are applied back and forth on the LO: the points are obtained from the measured population difference, whereas the solid line represents the LO phase measured after the correction phase actuator. The controller, implemented using coherence preserving measurements and feedback on a phase actuator, maintains the relative phase close to zero. Above the system is operated in open loop, below in closed loop. In the latter case, the phase corrections are applied  $150 \mu\text{s}$  after each measurement.

sition state in an atomic clock is based on the reconstruction of the phase drift experienced by the LO over the extended interrogation time  $T_{\text{tot}} = N \times T$  ( $N$  is the number of phase coherent interrogations) by combining the phase shifts applied by feedback and the final phase readout (Fig. 6). The known phase corrections applied to the LO phase serve the dual purpose of keeping the relative phase in the inversion region and giving a coarse estimate of the

phase drift during  $T_{\text{tot}}$ . The final phase measurement  $\varphi_f$ , together with the phase corrections  $\varphi_{\text{FB}}^{(i)}$ , gives a precise estimate of the phase drift during  $T_{\text{tot}}$ . The total phase drift can be computed as  $\varphi_{\text{tot}} = \varphi_f - \sum_{i=1}^N \varphi_{\text{FB}}^{(i)}$ , where the sum is over all the correction phase shifts applied by the feedback controller and stored in the microcontroller during the sequence. The feedback on the frequency is set accordingly to be  $\omega_{\text{FB}} = -\varphi_{\text{tot}}/T_{\text{tot}}$ . After the final phase read out, the phase shifter is reset to its initial position to avoid any impact of the intermediate phase shifts on the long term clock stability. The measurement SNR of the total phase drift depends only on the final phase measurement, since it can make use of all the residual ensemble coherence, whereas the SNR of the intermediate measurements has to be only sufficient to keep the atomic state in the inversion region. To further improve the protocol, the clock operation could be optimized by adapting the destructivity of the intermediate measurements to the varying coherence of the atomic sample, or implementing an adaptive measurement protocol for the last measurement [31].

For a proof-of-concept demonstration, we run an atomic clock that exploits the PLL between the LO and the atomic superposition state, and the phase reconstruction protocol. The LO signal was deteriorated so as to have an increased phase drift over the interrogation interval (see Appendix C). As a benchmark, we first run an atomic clock adopting a standard Ramsey interrogation sequence, and without any feedback on the phase. In the clock operation, the dead time for the preparation of the new ensemble is  $T_D = 1.9$  s and the interrogation time is set to  $T = 1$  ms, much shorter than the measured atomic coherence lifetime. The phase measurement is performed with the coherence preserving detection adopted for the phase lock. The two-sample Allan frequency standard deviation was calculated from the sum of the LO noise and the correction signal applied by the feedback controller. The clock instability reaches a  $\tau^{-1/2}$  scaling after a few clock cycles (see Fig. 7, red) at a level consistent with an initial SNR = 20 and considering the coherence decay in the optical trap. The instability is far higher than with state-of-the-art atomic clocks since the experimental setup was not explicitly designed for the operation of an atomic clock, and the Allan frequency standard deviation is  $1.5 \times 10^{-9}$  at 1 s. We then operate an atomic clock making use of a PLL sequence with  $N=9$  successive interrogations, and again with  $T=1$  ms, thus increasing the total interrogation time to 9 ms (see Fig. 6). For simplicity, the intermediate and the final phase readouts are set to have the same measurement strength. The Allan frequency deviation shows a  $\tau^{-1/2}$  scaling as expected for atomic clocks, which demonstrates that the phase reconstruction protocol is working properly. In the opposite case, frequency offsets would be corrected only at a short time with the phase actuator, and the stability of the clock would then diverge because of the non-zero dead time interval. The comparison of the instability shows that the clock adopting the phase lock and reconstruction

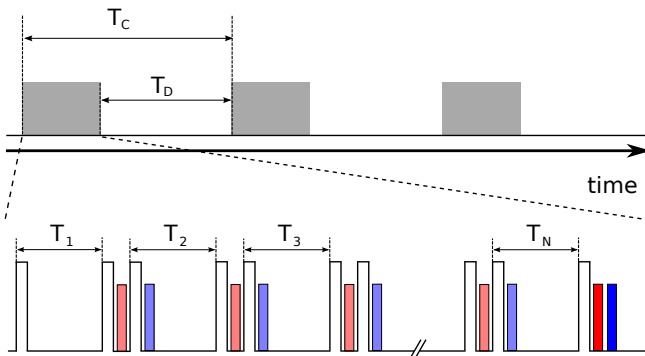


FIG. 6: **Protocol for atomic clock with PLL.** Operation of the clock: at each cycle of duration  $T_C$ , the relative phase is repeatedly measured in a coherence preserving way during the phase lock interval (above: shaded grey areas). Each interrogation, represented in the inset by a light red peak between the manipulation  $\pi/2$  pulses, is followed by a phase correction  $\varphi_{FB}^{(i)}$  on the LO, represented in the inset by a light blue peak in the right after the reintroduction of the spin on the equatorial plane of the Bloch sphere. The final phase readout  $\varphi_f$  (dark red peak in the inset), whose SNR is set by the residual coherence, together with the previously applied phase shifts on the LO, provides the total phase drift  $\varphi$  experienced during the extended interrogation interval  $T_{tot}=N \times T$ . The interrogation sequence ends with the application of a frequency correction on the LO (dark blue peak in the inset), then a new atomic ensemble is prepared in the dead time interval  $T_D$  for the next cycle.

method is at a lower level by a factor  $(4.76 \pm 0.25)$  with respect to the clock implementing the standard Ramsey interrogation, as shown in Fig. 7 (blue). In the optimal case, the instability would decrease by a factor 9 (Fig. 7, black line) because of the correspondingly longer interrogation time. Experimentally, we obtain a lower value because of several detrimental effects, where the main contributions are a reduced SNR due to the cumulated destructivity from the probe and the decay from the optical dipole trap, and the finite phase shifter accuracy, equal to 38 mrad. The result can be further compared to the case that the 9 phase measurements would have been uncorrelated, for example by repreparing the atomic state and starting a new Ramsey cycle after each measurement [32]. We would expect here a factor 3 (Fig. 7, black dashed line), which is clearly exceeded by the phase lock sequence.

The phase lock can be performed as long as the coherence of the state is maintained. For integration times longer than the coherence lifetime of the trapped ensemble, the atomic phase is lost and our locking scheme becomes again a frequency lock, like when the quantum superposition is destroyed by the detection. In our experiment, the coherence lifetime is limited to 20 ms by the dephasing in the optical dipole trap. Nevertheless, trapped induced dephasing of the atomic state can be

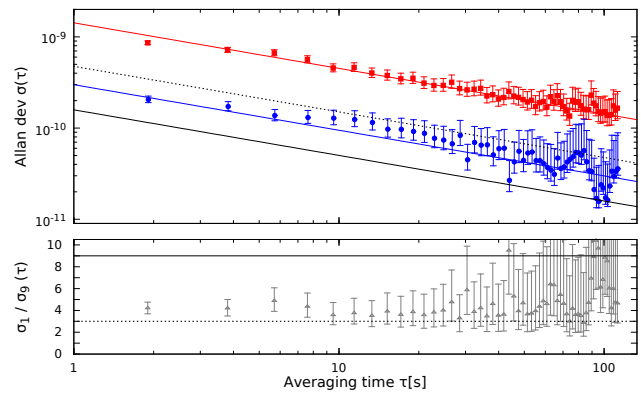


FIG. 7: **Atomic clock implementing a PLL.** (Top) Allan frequency standard deviation  $\sigma_1$  for a normal Ramsey clock with interrogation time  $T=1$  ms (red) and  $\sigma_0$  for a clock implementing the phase lock between the LO and the atomic superposition state for 9 successive, correlated interrogations on the same atomic ensemble, for a total interrogation time of  $9 \times T=9$  ms (blue). The dead time is in both cases  $T_D = 1.9$  s. The red and blue lines are fits to the data, with a slope set to  $\tau^{-1/2}$ . The continuous black line lies a factor 9 below the red curve, and represents the best achievable level of the phase lock sequence for the same number of interrogations. The dashed black line lies a factor 3 below the red curve, and is the optimum level for 9 consecutive uncorrelated Ramsey measurements with duration  $T$  each and the same total cycle time. (Bottom) The grey triangles represent the ratio of the Allan deviation for the two clocks; the solid and dashed lines correspond to the factors 9 and 3 from the top plot.

suppressed for  $^{87}\text{Rb}$  as reported in [16, 33], whereas in an optical lattice it is strongly reduced with the choice of light at the magic wavelength [34]. In the original proposal to lock the local oscillator phase on the atomic phase [25], frequency feedback on the local oscillator after each weak  $J_z$  measurement is performed. This scheme leads to a longer effective interrogation time, but to a SNR given by the weak measurements, which is lower than that of a measurement at the quantum projection noise and beyond. Our protocol can overcome this limit, and reach projection limited readout while keeping an extended interrogation time, thanks to the feedback on the LO phase.

In the phase lock sequence, several effects must be considered to maximize the SNR of the last measurement while maintaining a high accuracy on the total phase drift over the increased interrogation time: the rotations operated on the Bloch sphere must be fast, the measurement induced decoherence limited, and the phase shifter used for the correction accurate. The decoherence related to the repeated interrogations of the relative phase can be strongly reduced by the use of an optical cavity to enhance the probe interaction with the atomic ensemble [35–37]. An optimized clock configuration would consist in a two atomic ensembles using the same LO: the first ensemble provides the information to implement the phase feedback algorithm on the LO; the resulting cor-

rected phase for the LO stays in the inversion region for a much longer period, and this prestabilized LO is used to interrogate the master ensemble with the standard Ramsey sequence. This scheme avoids the requirement of a trade-off between the number of intermediate measurements and the SNR of the final measurement by separating the two problems. It also removes the systematics imposed by the intermediate coherent manipulations and measurements of the atomic state, which now affects only the first ensemble. The solution promises the same benefits foreseen for the phase reconstruction schemes proposed in [22, 23], but using only a single additional ensemble.

In an atomic clock the phase lock between the LO and the atomic superposition state can reduce the Dick effect [38], *i.e.* the aliasing of the clock oscillator, thanks to the longer interrogation time. However, the most important advantage of the scheme is the reduction of the decoherence related to the local oscillator, which translates to a lower white noise frequency for a fixed detection noise. The noise reduction can be exploited to lower the LO stability requirements to the benefit of other parameters, like portability of the experimental setup, for mobile or spatial applications, or viceversa, to remove the limitation set by the LO to reach ultimate performances.

For example, the interrogation interval in the best available optical clocks [12–15] is limited to  $\simeq 1$  s by the quality of the local oscillator; this limitation is not fundamental, and our method could increase the interrogation interval and hence the sensitivity in a way at best proportional to the number of coherence preserving interrogations. LOs with higher coherence will reduce the number of intermediate operations required to obtain a given clock interrogation interval. The latter will then be limited by other effects: practically, a first limit is set by the vacuum quality, which can reduce the ensemble coherence via background collisions, but extremely long trapping lifetimes have been already reached for trapped atoms [39]. Ultimately, with the combination of existing techniques and the method presented in this paper, the 1–10 mHz excited states lifetime expected for alkaline earth-like atoms could be reached, which motivates the search for transitions with a lower linewidth [40–42].

Phase locking the LO to the atomic state preserves classical correlations in time against the decoherence by the local oscillator. The technique and the related enhancement factor could thus be combined with spin squeezing, which improves the clock sensitivity by introducing quantum correlations between the particles to go below the standard quantum limit [37, 43]. More generally, increasing the interrogation time using minimally destructive measurements and feedback on the phase could be applied to other atomic interferometers, such as atomic inertial sensors, where for example the phase of the interrogation lasers could be locked to the phase evolution of matter waves.

In conclusion, using a coherence preserving detection we tracked the phase evolution of an atomic collective

superposition, and we reproduced it on a classical replica by introducing feedback to implement a PLL. Phase locking a classical oscillator to an atomic superposition state can be a key technology to improve the sensitivity of systems where the atomic phase evolution is used to improve the quality of the classical counterpart, such as in atomic interferometers or frequency combs [44], whenever the main decoherence source is determined by the classical subsystem. This development may open new directions and possibilities in several technological fields and as well in basic science.

### Acknowledgments

We acknowledge funding from DGA, CNES, EMRP (JRP-EXL01 QESOCAS), the European Union (EU) (iSENSE), ANR (MINIATOM), LAPHIA (APLL-CLOCK, within ANR-10-IDEX-03-02) and ESF EuroQUAM. The EMRP is jointly funded by the EMRP participating countries within EURAMET and the European Union. LCFIO and SYRTE are members of the Institut Francilien de Recherche sur les Atomes Froids (IFRAF). We thank T. Vanderbruggen for his contribution during the initial phase of the experiment, as well as M. Prevedelli, G. Santarelli and T. Udem for useful discussions. P.B. acknowledges support from a Chair of Excellence of Région Aquitaine, E.C. from Quantel. Any mention of commercial products does not constitute an endorsement.

### Appendix A: Atomic sample preparation

$^{87}\text{Rb}$  atoms laser cooled with a magneto-optical trap are transferred to an optical dipole trap at 1560 nm, that uses a 4 mirror optical resonator to enhance the laser intensity [45]. The atoms are trapped at the crossing of two cavity arms with a waist of 100  $\mu\text{m}$ . The ensemble is evaporatively cooled by decreasing the intensity of the dipole trap till a temperature of 10  $\mu\text{K}$  is reached for  $5 \times 10^5$  atoms in a cloud with  $1/e^2$  radius of 50  $\mu\text{m}$ . In the last operation before starting the Ramsey interrogation the atoms are optically pumped in the  $|\downarrow\rangle$  state. The sequence to prepare the ensemble in the initial state, which corresponds to the dead time  $T_D$  in the atomic clock sequence, lasts 1.9 s.

### Appendix B: Non-destructive dispersive probe

The measurement of  $J_z$  is based on the dispersion caused by the trapped atoms on a far off-resonance optical probe. The probe beam has a waist of 47  $\mu\text{m}$  matched to the size of the atomic cloud. It is phase modulated at a frequency of 3.853 GHz and frequency referenced at 3.377 GHz on the red of the the  $F=1 \rightarrow F'=2$  transition; these conditions produce a symmetric mixing of the  $|\downarrow\rangle$  and

$|\uparrow\rangle$  states because of probe induced spontaneous emission, thus avoiding a vertical offset when the Bloch sphere contracts. In this way, each sideband mainly probes the population of one of the two levels, with the same magnitude and opposite sign for the couplings. We cancel the probe induced light shift and the related decoherence by precisely compensating the effect of the carrier with that of the sidebands; the cancellation is obtained by setting a modulation depth of 14.8% for the phase modulation. The differential light-shift on the D2 line from the dipole trap at 1560 nm was compensated with light blue detuned from the  $5^2P_{3/2} \rightarrow 4^2D_{5/2,3/2}$  transitions at 1529 nm. When the total power of the probe is set to 480  $\mu\text{W}$ , it causes the decay of the atomic coherence with a lifetime of 2.85  $\mu\text{s}$ ; in the experiment here reported the interrogation pulses, obtained using an amplitude electro-optic modulator, have been set to last 60 ns. Each pulse determines then a 2% destructivity of the ensemble coherence, and a SNR of 20 for the  $J_z$  measurement on the initial sample of  $5 \times 10^5$  atoms. The population imbalance readouts have been normalized to the signal when all atoms were repumped to the state  $F=2$ .

### Appendix C: Frequency chain

The 6.835 GHz frequency used to coherently manipulate the atomic spin is generated by a frequency chain based on a Spectra Dynamics DLR-100 system as a frequency reference. The DLR-100 relies on an ultra-low noise 100 MHz quartz, locked at low frequency to the 10<sup>th</sup> harmonic of a frequency doubled 5 MHz quartz to further improve the phase noise. The 100 MHz signal is multiplied to 7 GHz and then mixed with a tunable synthesizer at 165 MHz to obtain the signal resonant with the transition between the  $|\downarrow\rangle$  and  $|\uparrow\rangle$  state. The noise added by the microwave pulses to the measurement of  $J_z$  is negligible for our weak probe, and its control well below the atomic quantum projection noise level has already been shown in [46]. Frequency noise is added to the LO signal using a frequency modulation port on the synthesizer, with a conversion factor set to 200 Hz/ $V_{\text{rms}}$ . The noise signal for the demonstration of the clock using the PLL sequence is generated with a signal generator, which produces white frequency noise with a spectral density of  $2.7 \times 10^{-2}$  Hz<sup>2</sup>/Hz; this signal is low pass filtered at 1.85 kHz before being added to the LO. The result is a rms phase drift of 430 mrad over 10 ms for the LO.

### Appendix D: Feedback controller

The atomic populations on the  $|\downarrow\rangle$  and  $|\uparrow\rangle$  states determine a differential phase shift of the probe sidebands. As a consequence, the probe beam is modulated in amplitude, and the modulation signal is detected by a photodiode (1591NF, New Focus), amplified (two HMC716LP3E, Hittite) and demodulated (ZX05-

73C-C+, Minicircuits). The electronic integration of this signal during the 60 ns interrogation pulse produces a voltage proportional to the average atomic population difference during the probing. Such a voltage is digitized by a 14 bit resolution analog-to-digital converter embedded in the microcontroller unit (MCU) used to control the feedback loop (ADuC841, Analog Devices). In the experiments implementing the phase lock between the LO and the atomic superposition the MCU controls the phase actuator, a 6 bits step phase shifter with a range of  $2\pi$  (RFPSHT0204N6, RF-Lambda). The total delay for the feedback is approximately 150  $\mu\text{s}$  depending on the calculation time of the MCU. When running the clock based on the PLL technique, the MCU acts as well on a frequency actuator, which is the frequency modulation input on the 165 MHz synthesizer.

The feedback controller we propose for the clock exploiting the phase lock between the LO and the atomic superposition state consists of a cycle divided in three main steps: in the first one, successive correlated interrogations with probe interval  $T$  are realized on the same coherent atomic ensemble, and feedback on the LO phase is applied. The control law is

$$\begin{aligned}\varphi_{\text{LO}}^{(i)} &= \varphi_{\text{LO}}^{(i-1)} + \varphi_{\text{FB}}^{(i)} \\ &= \varphi_{\text{LO}}^{(i-1)} + g_{\varphi}\varphi^{(i)}\end{aligned}$$

where  $\varphi^{(i)}$  is the estimated phase difference between the LO and the atoms at the  $i$ -th cycle and  $\varphi_{\text{LO}}^{(i)}$  is the phase of the LO only. The values of  $\varphi_{\text{FB}}^{(i)} = g_{\varphi}\varphi^{(i)}$  are saved in the feedback controller and typically a gain  $g_{\varphi} = -1$  is chosen.

The second step consists in the final phase readout: at the end of the  $N$ -th interrogation interval of duration  $T$ , a destructive measurement  $\varphi_f$  of the phase is performed, with the highest possible precision. The saved phase shifts on the LO and  $\varphi_f$  are used to reconstruct the full phase drift between the LO and the atoms in the total interrogation time, equal to  $T_{\text{tot}} = N \times T$ .

In the third step, one then performs feedback on the frequency as in a conventional atomic clock

$$\begin{aligned}\omega_{\text{LO}}^{(n)} &= \omega_{\text{LO}}^{(n-1)} + \omega_{\text{FB}}^{(n)} \\ &= \omega_{\text{LO}}^{(n-1)} + g_{\omega}\varphi_{\text{tot}}^{(n)}/T_{\text{tot}}\end{aligned}$$

where

$$\begin{aligned}\varphi_{\text{tot}}^{(n)} &= \varphi_f^{(n)} - \sum_{i \in n\text{-th cycle}} \varphi_{\text{FB}}^{(i)} \\ &= \varphi_f^{(n)} - \sum_{i \in n\text{-th cycle}} g_{\varphi}\varphi^{(i)}\end{aligned}$$

and  $n$  is the clock cycle. In addition, the phase shift set by the feedback controller on the LO is reset to zero

$$\varphi_{\text{LO}}^{(n)} = \varphi_{\text{LO}}^{(0)} = 0.$$

The cycle then repeats. The important feature of the feedback controller is that the feedback actions on the LO

oscillator phase during the interrogation time are saved. They are then used with the output of the final precise measurement to determine the total phase drift. There is no drawback from the uncertainty of the weak measurements, since any feedback errors are detected with

the precise final measurement at the end. As already remarked, in the experimental demonstration of the clock operation, we adopted the same probe for the intermediate and the final measurements.

- 
- [1] C. Huygens, *Œuvres Complètes de Christiaan Huygens*, vol. 15 (M. Nijhoff, The Hague, 1893).
- [2] A. Mari, A. Farace, N. Didier, V. Giovannetti, and R. Fazio, *Measures of quantum synchronization in continuous variable systems*, Phys. Rev. Lett. **111**, 103605 (2013).
- [3] M. Xu, D. A. Tieri, E. C. Fine, J. K. Thompson, and M. J. Holland, *Synchronization of Two Ensembles of Atoms*, Phys. Rev. Lett. **113**, 154101 (2014).
- [4] K. C. Cox, J. M. Weiner, and J. K. Thompson, *Phase diagram for injection locking a superradiant laser*, Phys. Rev. A **90**, 053845 (2014).
- [5] H. Guan-Chyun and J. C. Hung, *Phase-locked loop techniques. a survey*, IEEE Tans. Ind. Electron. **43**, 609 (1996).
- [6] D. J. Jones, S. A. Diddams, J. K. Ranka, A. Stentz, R. S. Windeler, J. L. Hall, and S. T. Cundiff, *Carrier-envelope phase control of femtosecond mode-locked lasers and direct optical frequency synthesis*, Science **288**, 635 (2000).
- [7] S. A. Diddams, D. J. Jones, J. Ye, S. T. Cundiff, J. L. Hall, J. K. Ranka, R. S. Windeler, R. Holzwarth, T. Udem, and T. W. Hänsch, *Direct link between microwave and optical frequencies with a 300 thz femtosecond laser comb*, Phys. Rev. Lett. **84**, 5102 (2000).
- [8] R. Slavík, F. Parmigiani, J. Kakande, C. Lundström, M. Sjödin, P. A. Andrekson, R. Weerasuriya, S. Sygletos, A. D. Ellis, L. Gruner-Nielsen, et al., *All-optical phase and amplitude regenerator for next-generation telecommunications systems*, Nat. Photonics **4**, 690 (2010).
- [9] M. S. Braasch and A. J. V. Dierendonck, *GPS receiver architectures and measurements*, Proc. IEEE **87**, 48 (1999).
- [10] M. Arndt, *De Broglie's meter stick: making measurements with matter waves*, Phys. Today **67**, No. 5, 30 (2014).
- [11] C. W. Chou, D. B. Hume, J. C. J. Koelemeij, D. J. Wineland, and T. Rosenband, *Frequency comparison of two high-accuracy Al<sup>+</sup> optical clocks*, Phys. Rev. Lett. **104**, 070802 (2010).
- [12] N. Hinkley, J. A. Sherman, N. B. Phillips, M. Schioppa, N. D. Lemke, K. Beloy, M. Pizzocaro, C. W. Oates, and A. D. Ludlow, *An atomic clock with 10<sup>-18</sup> instability*, Science **341**, 1215 (2013).
- [13] B. J. Bloom, T. L. Nicholson, J. R. Williams, S. L. Campbell, M. B. X. Zhang, W. Zhang, S. L. Bromley, and J. Ye, *An optical lattice clock with accuracy and stability at the 10<sup>-18</sup> level*, Nature **506**, 71 (2014).
- [14] I. Ushijima, M. Takamoto, M. Das, T. Ohkubo, and H. Katori, *Cryogenic optical lattice clocks*, Nat. Photonics **9**, 185 (2015).
- [15] T. L. Nicholson, S. L. Campbell, R. B. Hutson, G. E. Marti, B. J. Bloom, R. L. McNally, W. Zhang, M. D. Barrett, M. S. Safronova, G. F. Strouse, W. L. Tew, and J. Ye, *2×10<sup>-18</sup> total uncertainty in an atomic clock*, arXiv:1412.8261 [physics.atom-ph].
- [16] G. Kleine Büning, J. Will, W. Ertmer, E. Rasel, J. Arlt, C. Klempt, F. Ramirez-Martinez, F. Piéchon, and P. Rosenbusch, *Extended coherence time on the clock transition of optically trapped rubidium*, Phys. Rev. Lett. **106**, 240801 (2011).
- [17] Y. Y. Jiang, A. D. Ludlow, N. D. Lemke, R. W. Fox, J. A. Sherman, L.-S. Ma, and C. W. Oates, *Making optical atomic clocks more stable with 10<sup>-16</sup>-level laser stabilization*, Nat. Photonics **5**, 158 (2011).
- [18] T. Kessler, C. Hagemann, C. Grebing, T. Legero, U. Sterr, F. Riehle, M. J. Martin, L. Chen, and J. Ye, *A sub-40-mHz-linewidth laser based on a silicon single-crystal optical cavity*, Nat. Photonics **6**, 687 (2012).
- [19] M. J. Thorpe, L. Rippe, T. M. Fortier, M. S. Kirchner, and T. Rosenband, *Frequency stabilization to 6×10<sup>-16</sup> via spectral-hole burning*, Nat. Photonics **5**, 688 (2011).
- [20] G. D. Cole, W. Zhang, M. J. Martin, J. Ye, and M. Aspelmeyer, *Tenfold reduction of Brownian noise in high-reflectivity optical coatings*, Nat. Photonics **7**, 644 (2013).
- [21] S. Amairi, T. Legero, T. Kessler, U. Sterr, J. B. Wubbena, O. Mandel, and P. O. Schmidt, *Reducing the effect of thermal noise in optical cavities*, Appl. Phys. B **113**, 233 (2013).
- [22] T. Rosenband and D. R. Leibbrandt, *Exponential scaling of clock stability with atom number*, arXiv:1303.6357 [quant-ph].
- [23] E. M. Kessler, P. Kómár, M. Bishof, L. Jiang, A. S. Sørensen, J. Ye, and M. D. Lukin, *Heisenberg-limited atom clocks based on entangled qubits*, Phys. Rev. Lett. **112**, 190403 (2014).
- [24] J. Borregaard and A. S. Sørensen, *Efficient atomic clocks operated with several atomic ensembles*, Phys. Rev. Lett. **111**, 090802 (2013).
- [25] N. Shiga and M. Takeuchi, *Locking the local oscillator phase to the atomic phase via weak measurement*, New J. Phys. **14**, 023034 (2012).
- [26] N. Shiga, M. Mizuno, K. Kido, P. Phoonthong, and K. Okada, *Accelerating the averaging rate of atomic ensemble clock stability using atomic phase lock*, New J. Phys. **16**, 073029 (2014).
- [27] We remark that an unambiguous determination of the LO phase drift beyond the inversion region could be obtained by tracking its evolution with periodic measurements of two orthogonal projections of the phase, at least when the Bloch vector is close to the borders of the inversion region. This solution does not require the phase lock protocol, but brings an increase in the number of interrogations of the atomic sample, and hence of the probe induced destructivity.
- [28] T. Vanderbruggen, R. Kohlhaas, A. Bertoldi, S. Bernon, A. Aspect, A. Landragin, and P. Bouyer, *Feedback control of trapped coherent atomic ensembles*, Phys. Rev. Lett.



- 110**, 210503 (2013).
- [29] G. A. Smith, A. Silberfarb, I. H. Deutsch, and P. S. Jessen, *Efficient quantum-state estimation by continuous weak measurement and dynamical control*, Phys. Rev. Lett. **97**, 180403 (2006).
- [30] S. Lloyd and J.-J. E. Slotine, *Quantum feedback with weak measurements*, Phys. Rev. A **62**, 012307 (2000).
- [31] J. Borregaard and A. S. Sørensen, *Near-Heisenberg-limited atomic clocks in the presence of decoherence*, Phys. Rev. Lett. **111**, 090801 (2013).
- [32] J. Lodewyck, P. G. Westergaard, and P. Lemonde, *Non-destructive measurement of the transition probability in a Sr optical lattice clock*, Phys. Rev. A **79**, 061401(R) (2009).
- [33] A. G. Radnaev, Y. O. Dudin, R. Zhao, H. H. Jen, S. D. Jenkins, A. Kuzmich, and T. A. B. Kennedy, *A quantum memory with telecom-wavelength conversion*, Nat. Phys. **6**, 894 (2010).
- [34] H. Katori, M. Takamoto, V. G. Pal'chikov, and V. D. Ovsianikov, *Ultrastable optical clock with neutral atoms in an engineered light shift trap*, Phys. Rev. Lett. **91**, 173005 (2003).
- [35] J. G. Bohnet, K. C. Cox, M. A. Norcia, J. M. Weiner, Z. Chen, and J. K. Thompson, *Reduced spin measurement back-action for a phase sensitivity ten times beyond the standard quantum limit*, Nat. Photonics **8**, 731 (2014).
- [36] J. Lee, G. Vrijsen, I. Teper, O. Hosten, and M. A. Kasevich, *Many-atom-cavity QED system with homogeneous atom-cavity coupling*, Opt. Lett. **39**, 4005 (2014).
- [37] I. D. Leroux, M. H. Schleier-Smith, and V. Vuletić, *Implementation of cavity squeezing of a collective atomic spin*, Phys. Rev. Lett. **104**, 073602 (2010).
- [38] G. J. Dick, J. D. Prestage, C. A. Greenhall, and L. Maleki, *Local oscillator induced degradation of medium-term stability in passive atomic frequency standards*, Proceedings of the 22<sup>nd</sup> Precise Time and Time Interval (PTTI) Applications and Planning Meeting, Vienna, Virginia, USA (NASA CP-3116) pp. 487–508 (1990).
- [39] P. A. Willems and K. G. Libbrecht, *Creating long-lived neutral-atom traps in a cryogenic environment*, Phys. Rev. A **51**, 1403 (1995).
- [40] C. J. Campbell, A. G. Radnaev, A. Kuzmich, V. A. Dzuba, V. V. Flambaum, and A. Derevianko, *Single-ion nuclear clock for metrology at the 19th decimal place*, Phys. Rev. Lett. **108**, 120802 (2012).
- [41] A. Derevianko, V. A. Dzuba, and V. V. Flambaum, *Highly charged ions as a basis of optical atomic clockwork of exceptional accuracy*, Phys. Rev. Lett. **109**, 180801 (2012).
- [42] A. Kozlov, V. A. Dzuba, and V. V. Flambaum, *Prospects of building optical atomic clocks using ErI and ErIII*, Phys. Rev. A **88**, 032509 (2013).
- [43] A. Louchet-Chauvet, J. Appel, J. J. Renema, D. Oblak, N. Kjørgaard, and E. S. Polzik, *Entanglement-assisted atomic clock beyond the projection noise limit*, New J. Phys. **12**, 065032 (2010).
- [44] A. Cadarso, J. Mur-Petit, and J. J. García-Ripoll, *Phase Stabilization of a Frequency Comb using Multi-pulse Quantum Interferometry*, Phys. Rev. Lett. **112**, 073603 (2014).
- [45] S. Bernon, T. Vanderbruggen, R. Kohlhaas, A. Bertoldi, A. Landragin, and P. Bouyer, *Heterodyne non-demolition measurements on cold atomic samples: towards the preparation of non-classical states for atom interferometry*, New J. Phys. **13**, 065021 (2011).
- [46] Z. Chen, J. G. Bohnet, J. M. Weiner, and J. K. Thompson, *A low phase noise microwave source for atomic spin squeezing experiments in <sup>87</sup>Rb*, Rev. Sci. Instrum. **83**, 044701 (2012).